THE ASTROPHYSICAL JOURNAL, 407:699–713, 1993 April 20

THE ABUNDANCE OF LITHIUM IN METAL-POOR SUBGIANT STARS

C. A. PILACHOWSKI
Kitt Peak National Observatory, National Optical Astronomy Observatories,[1] P.O. Box 26732, Tucson, AZ 85726-6732
C. SNEDEN
Department of Astronomy and McDonald Observatory, University of Texas, Austin, TX 78712
AND
J. BOOTH[2]
Lick Observatory, University of California at Santa Cruz, Santa Cruz, CA 95064
Received 1992 June 26; accepted 1992 October 23

ABSTRACT

We have determined lithium abundances for a sample of 79 halo subgiants. The subgiant candidates were identified using *uvby* photometry from several catalogs of metal-poor stars. The basic data were high-resolution, low-noise coudé spectra in the 6700 Å spectral region. Abundances of iron and calcium, derived from one Ca I and several Fe I lines in our spectra, provided a metallicity discriminant for the stars in our sample. The subgiants with temperatures between 5500 and 4900 K show a steady decline of lithium abundance with advancing subgiant position (and decreasing temperature). The observed trend is in qualitative agreement with recent theoretical models of lithium dilution in metal-poor stars, especially if main-sequence diffusion is included. The initial lithium abundances in metal-poor stars may have been slightly larger than that exhibited by stars near the main-sequence turnoff. For stars with temperatures below 4900 K, the models predict no further dilution, but observed lithium abundances continue to decline with decreasing temperature, indicating further lithium destruction on the giant branch of metal-poor stars. In all postdilution subgiants, the observed lithium abundances show more scatter than do stars at the main-sequence turnoff, suggesting variations in the main-sequence lithium destruction below the observable surface layers.

Subject headings: stars: abundances — stars: Population II

1. INTRODUCTION

A decade ago Spite & Spite (1982) discovered that lithium in unevolved metal-poor stars near the main-sequence turnoff is present at a level of about one-tenth of the observed abundance in young Population I stars and in the interstellar medium. Since that time numerous investigators (Spite, Maillard, & Spite 1984; Hobbs & Duncan 1987; Rebolo, Molaro, & Beckman 1988, hereafter RMB; Hobbs & Thorburn 1991) have contributed to a growing body of observations establishing that halo subdwarfs near the main-sequence turnoff (i.e., above a temperature of about 5800 K and more metal-poor than [Fe/H] = −1.0;[3] cf. RMB) show the same surface lithium abundance, largely independent of temperature or metallicity, even in the most extreme metal-poor stars. Spite et al. (1991) summarize the Li observations in very metal-poor dwarfs, and suggest that the Li abundance plateau in dwarfs extends throughout the temperature range 6400 K $\geq T_{\rm eff} \geq$ 5500 K. Hobbs, Welty, & Thorburn (1991) have identified one apparent metal-poor subdwarf, G186−26, with a lithium abundance much below the plateau value of log ϵ(Li) = 2.1. Dearborn, Schramm, & Hobbs (1992) have postulated the existence of a lithium dip along the Population II main sequence similar to the dip on the Population I main sequence. Such stars must, however, be relatively rare, judging by the otherwise narrow distribution of lithium abundances among subdwarfs at the turnoff.

The near-uniformity in the surface lithium abundance among the subdwarfs has led a number of workers to postulate that the lithium found in Population II stars was formed in the big bang rather than in the stars or in the early Galaxy. On the other hand, some theoretical investigations have suggested that the amount of lithium presently observed in halo stars may have been depleted over time from an initially higher value in a manner leading to the observed uniformity (Deliyannis, Demarque, & Kawaler 1990; Proffitt & Michaud 1991). The initial value of the lithium abundance from the big bang remains an open question, but the uniformity in the surface lithium abundance in Population II stars at the main-sequence turnoff, with one or two notable exceptions, is observationally well established.

Iben (1965) originally investigated the changes in the stellar lithium abundance during main-sequence evolution and beyond. On the main sequence, low-mass stars retain lithium only on the surface, about 1%–2% by mass. Beneath the surface the temperature is too hot for lithium to survive; lithium nuclei rapidly react with protons to form beryllium. Low-mass stars leaving the main sequence when hydrogen is depleted in their cores develop surface convection zones, which deepen as the star continues to evolve to lower surface temperature. The surface convection zone mixes the surface layer with deeper material in which the lithium has been depleted. This dilution of the surface layer causes the observed surface lithium abundance to fall. The amount of dilution depends on

[1] Operated by the Association of Universities for Research in Astronomy, Inc. (AURA) under cooperative agreement with the National Science Foundation.
[2] Visiting Observer, Kitt Peak National Observatory, operated by the Association of Universities for Research in Astronomy, Inc. (AURA) under cooperative agreement with the National Science Foundation.
[3] We adopt two standard spectroscopic notations in this paper. First, $[X] \equiv \log_{10}(X)_{\rm star} - \log_{10}(X)_{\rm sun}$ for any abundance quantity X. Second, $\log \epsilon(X) \equiv \log(N_X/N_{\rm H}) + 12.0$ for absolute number density abundances.

how deep the convective zone penetrates. A detailed investigation of the dilution of lithium during subgiant evolution can provide quantitative estimates of the thickness of the lithium layer at the end of the main-sequence lifetime, the rate at which the convective zone deepens, and the ultimate fraction of the star's mass which is contained in the convective zone.

Halo subgiants are a particularly simple population is which to study lithium dilution. Considering only those stars more metal-poor than [Fe/H] < -1.4, the range in the age of formation is relatively small compared to the age of the Galaxy. Unlike the Population I subgiants, the halo subgiants evolve from a restricted range of mass on the main sequence. The age, mass, and evolutionary phase of the sample can therefore be rather tightly constrained. The remaining parameter which can vary widely is overall metal abundance, but the metallicity can be determined with comparative ease.

Star clusters offer the best approach for this study, since subgiants can be easily identified from color-magnitude diagrams. Open clusters contain too few subgiants, however, and the globular cluster subgiants are too distant and too faint for quantitative high resolution spectroscopy. Additionally, at least some globular clusters are chemically inhomogeneous in the light elements even down to the main sequence. Briley, Hesser, & Bell (1991) demonstrate fairly convincingly that C and N variations occur in unevolved stars of 47 Tucanae, indicating the possible existence of chemical self-pollution in globular clusters.

The field halo subgiants provide several advantages, beginning with uniform and known age and mass. They probably have homogeneous primordial abundance mixes except for a couple of known anomalous stars, and they are bright enough and numerous enough that we can observe a reasonable sample. From previous work (see above), we know that their surface lithium abundances at the main-sequence turnoff are remarkably uniform. Of course, the main problem in dealing with this or any other sample of field stars lies in the determination of absolute magnitudes.

In this paper we describe the identification of halo subgiants and determine their lithium abundances and overall metallicities in order to study quantitatively the problems of lithium dilution and the formation of the convective envelope in low-mass, metal-poor stars.

2. THE IDENTIFICATION OF HALO SUBGIANTS

Halo subgiants can be distinguished from subdwarfs and from horizontal-branch stars based on their luminosity. Parallaxes can be used to determine distances, and, hence, absolute luminosities, and colors or spectral types can also provide information about luminosity. Strömgren photometry is particularly appropriate for determining the luminosity (or evolutionary phase) and temperature of stars in this part of the Hertzsprung-Russell diagram (see the careful discussions and calibrations of Bond 1970, 1980, and of Crawford 1975). Extensive collections of Strömgren photometry of potential halo stars are available in the literature.

To produce the initial list of candidate metal-poor subgiants, we made use of the catalog of halo subdwarfs of Laird, Carney, & Latham (1988, hereafter LCL), the catalog of halo giants of Bond (1980), and the series of papers on high-velocity stars of Schuster & Nissen (1988, 1989a, 1989b). Each of these references contains extensive Strömgren photometry of halo stars. Stars were selected from these catalogs based on two criteria. We included only stars with $b - y > 0.3$, and we included stars with $\Delta m_1 > 0.12$. The latter criterion is imposed to restrict the sample of stars included to those likely to be metal-poor. The calibrations of Δm_1 versus [Fe/H] available include those of Bond (1980), Schuster & Nissen (1989a), and Olsen (1984). A lower limit of 0.12 on Δm_1 restricts the sample to those stars more metal-poor than approximately [Fe/H] $= -1.4$, depending on the specific calibration adopted. This limit of [Fe/H] < -1.4 has been chosen from our inspection of Figure 3 of RMB. In this figure, unevolved stars more metal-rich than [Fe/H] $= -1.4$, show a range of lithium abundances, but for stars more metal-poor, the lithium abundance is generally very near log ϵ(Li) = 2.1. By restricting the sample of stars we consider to [Fe/H] < -1.4, we can adopt the assumption that the surface lithium abundance at the end of the main sequence lifetime is log ϵ(Li) = 2.1. This allows us to assume that any subgiant lithium abundances below this value can be attributed to convective dilution in the stellar envelopes of these evolving stars.

The stars selected using the above criteria can be plotted in a c_1 versus $b - y$ diagram, as shown in Figure 1. The Strömgren c_1 index is a luminosity indicator, and $b - y$ is, of course, an indicator of temperature, so a plot of c_1 versus $b - y$ does portray an H-R diagram for our sample of metal-poor stars. Note that the indices plotted in Figure 1 are not corrected for reddening; while $b - y$ is obviously sensitive to reddening, the sensitivity of c_1 to reddening is quite small. For most stars in Figure 1, reddening will not affect the determination of evolutionary phase. The exception is for stars very near the main-sequence turnoff, where subgiants and main-sequence stars differ in color but have similar c_1 indices.

The three catalogs from which we have drawn our sample include metal-poor stars at all phases of evolution from the main sequence through the horizontal branch. The main sequence, subgiant branch, giant branch, and horizontal branch are discriminated clearly in Figure 1, and we have indicated the loci of these branches with a dotted line in the figure. The structure of the evolutionary sequence near the main sequence is most clearly delineated in the data of Schuster &

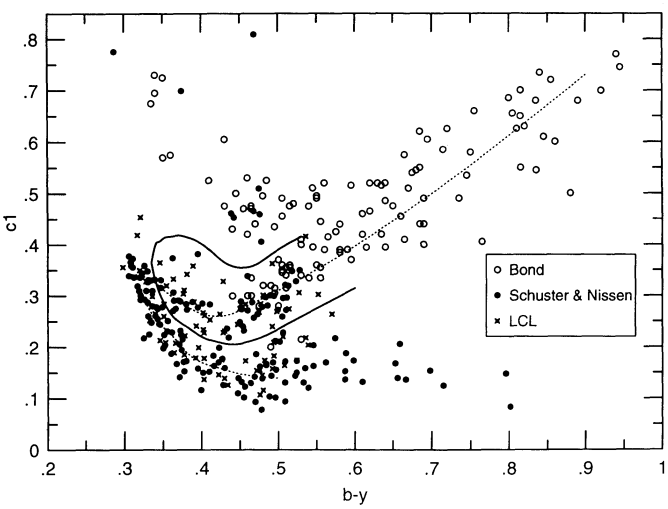

FIG. 1.—A Strömgren photometry color-magnitude diagram for candidate stars. The *uvby* catalogs employed for this figure are identified in the inset. We have included here only stars with $b - y > 0.30$ and $\Delta m_1 > 0.12$. The dashed line is a free-hand representation of the metal-poor star color-magnitude diagram defined by these data. The solid line loop indicates the positions of most of our candidate stars.

Nissen (1988). We can use this diagram to identify which of the metal-poor stars selected on the basis of $b - y$ and Δm_1 are, in fact, subgiants. The sample we finally select for lithium abundance determinations is defined mostly by those stars contained within the solid line loop in Figure 1. This loop is open at its high $b - y$ end to indicate that we have included some giants from the list of Bond (1980), in order to explore the behavior of lithium as the stars evolve up the giant branch. This list is given in Table 1, complete with determinations from the literature of temperature, gravity, microturbulent velocity, and [Fe/H]. Two stars from Bond's list, BD +4°2466 and BD −1°2582, have c_1 indices which place them in the regime of the subdwarfs. Bond argues that c_1 is depressed by strong CH apparent in his objective prism spectra, and that these stars are giants, not subdwarfs. We have included these two stars in our sample. Finally, for comparison to our subgiant sample we also include in Table 1 several metal-poor stars at the main-sequence turnoff with Li abundances already reported in the literature.

Where available, the parallaxes of our target stars offer an opportunity to confirm whether these stars are indeed subgiants. Parallaxes are available for 20 stars from Table 1 from van Altena, Lee, & Hoffleit (1991). For one star, HD 140283, we have adopted a more recently determined parallax measurement from Dahn (1992). The new parallax measurement of $\pi = 0.0150 \pm 0.0023$ (m.e.), leads to an absolute V magnitude of 3.09 ± 0.33. This absolute magnitude clearly places HD 140283 on the subgiant branch, consistent with both the Strömgren colors and the spectroscopic surface gravity determined by Magain (1985) and Gilroy et al. (1988).

The absolute V magnitudes determined from the parallaxes are plotted versus effective temperature in Figure 2, along with evolutionary tracks from VandenBerg (1992). (The tracks are computed at [Fe/H] values of −1.26 and −0.78, and at 0.8 and 0.85 solar masses, respectively.) Generally, the parallax data confirm our assignments of evolutionary phase based on Strömgren colors, especially for those stars cooler than about 5200 K. The parallaxes of a majority of the warmer stars are also consistent with our assignments (recall that we have included a few subdwarfs near the turnoff for comparison with other studies).

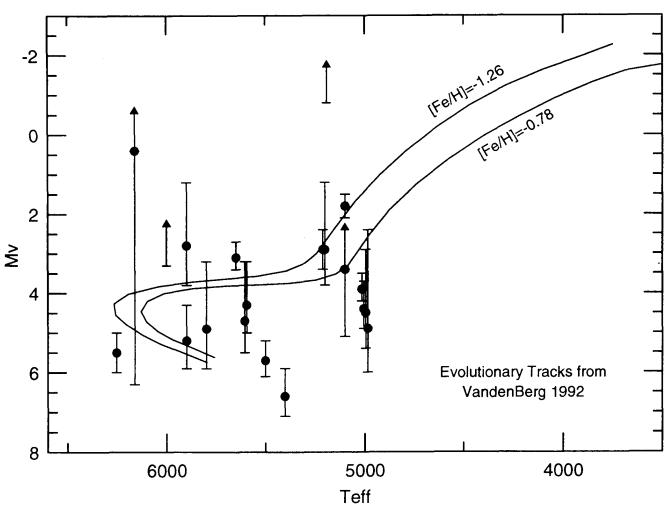

FIG. 2.—The absolute magnitudes of stars with available parallax data are plotted vs. effective temperature. For a few stars, the uncertainty in the parallax is larger than the measured parallax, and the absolute magnitude has been plotted as a "lower" limit. Two stellar evolution tracks from VandenBerg (1992) are included for stars with [Fe/H] = −1.26 and −0.78 and $M = 0.8$ and $0.85 M_{\rm Sun}$, respectively.

In a few cases, the evolutionary phase suggested by the parallax is inconsistent with the photometry or ambiguous. Three stars, HD 132475, HD 160617, and HD 163810, have parallaxes which are too large for these stars to be subgiants, but the Strömgren colors of these stars place them clearly past the main-sequence turnoff in the subgiant regime. In four other stars, HD 94028, HD 189558, HD 201889, and BD +72°94, the uncertainty in the parallax measurement is large enough to be consistent with either subdwarf or subgiant status. We will treat these stars as subgiants but caution the reader that some uncertainties will exist in their evolutionary status. Excepting HD 132475, the inconsistent/ambiguous stars have temperatures too hot for convective envelope formation or metallicities too high to include as "halo" stars, and so have no bearing on our conclusions. Generally the astrometric parallax data offer strong confirmation that our candidates are indeed subgiants.

Finally, the very small (and reasonably well-determined) parallax of HD 175305 suggests the star is more luminous than a subgiant, while the Strömgren colors and spectroscopic gravities place the star unambiguously in the subgiant regime. An oblique indication of the evolutionary status of HD 175305 is suggested by its carbon isotope ratio. Sneden, Pilachowski, & VandenBerg (1986) derived $^{12}C/^{13}C \simeq 40$ for this star, the highest isotope ratio of any of the field giants that they studied (most giants in their sample exhibited $^{12}C/^{13}C \leq 10$). They argued that the high $^{12}C/^{13}C$ of HD 175305 indicated that this star is much less internally mixed, and therefore less evolved and less luminous, than the typical field metal-poor giant.

3. OBSERVATIONS

Spectra of the λ6707 Å feature of Li I in most of our program stars were obtained using the coudé feed telescope and coudé spectrograph at the Kitt Peak National Observatory between 1988 November and 1989 November. The spectra were taken with camera 5, grating "A", and a Texas Instruments CCD designated "TI2." The dispersion was typically 0.11 Å pixel^{-1}, the spectrograph entrance slit was set to project to 2 pixels, and measurements of the widths of lines of thorium-argon spectra with this setup confirmed that the resolution was $R \simeq 30{,}000$. The signal-to-noise ratio per pixel of the resulting spectra was between 100 and 300. The spectral coverage usually included the Fe I line at 6678 Å through the Fe I line at 6750 Å. We used the IRAF software package to reduce the data from the raw CCD images through the steps of bias subtraction, flat-field correction, spectrum extraction, continuum fitting, and wavelength calibration using a thorium argon lamp spectrum.

Following complete data reduction, the wavelengths of key spectral features were measured: four Fe I lines and one Ca I line were considered in addition to the Li I doublet. In spectra of moderately metal-poor stars, only these few lines are visible; in some of the most metal-poor stars, only the Li I feature is seen. In Figure 3 we present the spectra of three typical program stars, chosen to indicate the range of line strengths seen in our data. The Li I feature, invisible in the spectrum of the relatively metal rich star HD 18907, becomes the only obvious feature in the spectrum of the very metal-poor star G20−8 (the Fe I line at 6678 Å probably is present, but it is not significantly stronger than noise features in this spectrum). In spectra with other lines present, the wavelengths of those

TABLE 1

LITERATURE DATA FOR PROGRAM STARS

Star	V	b−y	m_1	c_1	ref	T_{eff}	log g	v_{turb}	[Fe/H]	ref
HD 97	9.7	0.51	0.15	0.35	1	...	...	...	−1.50	1
						5015	...	...	−1.50	2
HD 2665	7.7	0.54	0.09	0.34	1	...	...	...	−2.30	1
						5000	2.50	2.4	−1.99	3
						5120	3.00	2.0	−1.69	4
						4980	...	...	−2.05	2
HD 4306	9.0	0.52	0.05	0.35	5, 1	...	...	...	−2.70	1
						5000	1.75	2.0	−2.70	6
						5000	1.50	1.8	−2.65	7
						4950	2.10	2.0	−2.92	8
						5000	2.25	2.0	−2.83	9
						...	...	...	−2.80	10
						4930	...	...	−2.45	2
HD 4906	8.8	0.48	0.22	0.30	5	...	...	...	...	...
HD 5426	9.6	0.50	0.08	0.34	1	...	...	...	−2.30	1
HD 6755	7.7	0.49	0.12	0.28	5, 1	...	...	...	−1.70	1
						5200	2.50	2.4	−1.56	3
						5260	3.00	2.7	−1.67	4
						...	...	...	−1.58	10
						5200	...	...	−1.80	2
HD 18907	5.9	0.51	0.23	0.32	5	...	...	...	...	...
HD 21581	8.7	0.56	0.14	0.34	1	...	...	...	−1.80	1
						4750	...	...	−1.66	2
HD 24289	10.0	0.39	0.05	0.29	5	...	...	...	−1.64	10
HD 24616	6.7	0.51	0.25	0.32	5	...	...	...	...	...
HD 44007	8.1	0.56	0.14	0.35	1	...	...	...	−1.70	1
						...	...	...	−1.70	11
HD 45282	8.0	0.45	0.11	0.28	5	...	...	...	−1.51	10
HD 76932	5.8	0.35	0.12	0.30	5	5860	3.50	...	−1.10	12
						5630	3.88	0.8	−1.01	4
						5810	3.50	...	−1.12	13
HD 84937	8.3	0.30	0.06	0.35	5,14	6200	...	...	−2.10	15
						6250	...	...	−2.18	16
						6216	...	...	−2.42	14
						6240	...	...	−2.13	17
						...	...	...	−2.14	10
						6200	3.60	1.5	−2.43	18
						6250	4.00	...	−2.10	12
HD 87140	9.0	0.48	0.12	0.28	5	5000	4.50	1.0	−1.41	4
						...	...	...	−1.56	10
HD 88609	8.6	0.68	0.09	0.54	1	...	...	...	−2.50	1
						4500	1.10	2.8	−2.77	3
						4500	0.80	3.2	−2.65	7
						4600	...	...	−2.75	2
HD 94028	8.2	0.34	0.08	0.25	5	5795	4.00	...	−1.70	12
						5860	...	...	−1.70	15
						5910	3.80	...	−1.76	13
						5800	...	...	−1.67	16
						5902	...	...	−1.50	14
						5900	...	...	−1.57	17
						...	...	...	−1.32	10
HD 97916	9.2	0.29	0.10	0.41	5	6125	4.00	...	−1.10	12
						6160	...	...	−1.39	17
						6240	3.70	...	−1.28	13
						5950	...	...	−1.50	16
						6204	...	...	−1.36	14
HD 101063	9.4	0.50	0.15	0.27	5	...	...	...	−1.35	10
HD 107752	10.0	0.58	0.09	0.39	1	...	...	...	−2.60	1
						4750	0.80	2.7	−2.54	7
						4775	...	...	−2.70	2

TABLE 1—*Continued*

Star	V	b−y	m_1	c_1	ref	T_{eff}	log g	v_{turb}	[Fe/H]	ref
HD 108317	8.1	0.44	0.06	0.30	1	...	...	...	−2.30	1
						5000	2.30	1.5	−2.29	7
						5200	2.50	1.5	−2.20	3
						5125	...	...	−2.35	2
HD 111721	8.0	0.51	0.18	0.30	1	...	...	...	−1.11	10
						5100	2.90	1.0	−1.25	19
HD 115444	9.0	0.57	0.07	0.43	1	...	...	...	−2.70	1
						4800	2.00	2.2	−2.64	3
						4750	...	...	−2.65	2
HD 122563	6.2	0.64	0.09	0.52	1	...	...	...	−2.60	1
						4600	0.80	3.2	−2.59	6
						4600	1.40	2.8	−2.35	7
						4640	1.30	2.0	−2.38	4
						4600	1.20	2.3	−2.45	3
						4500	0.75	2.5	−2.93	9
						4650	...	...	−2.75	2
						4615	1.20	1.5	−2.71	19
HD 126587	9.1	0.60	0.05	0.37	1	...	...	...	−2.70	1
						4750	1.10	2.0	−2.66	7
HD 128279	8.0	0.47	0.05	0.28	1	...	...	...	−2.50	1
						5000	2.20	1.4	−2.19	3
						5125	2.20	2.0	−2.50	9
HD 132475	8.6	0.40	0.06	0.28	5,14	5542	...	...	−1.93	14
						5550	...	...	−1.60	20
						5600	...	...	−2.16	17
						...	...	...	−1.32	10
HD 134169	7.7	0.38	0.12	0.31	14	5800	3.80	...	−1.60	12
						5750	...	...	−1.49	17
						5720	3.60	0.5	−0.97	19
						5750	4.50	1.0	−1.02	4
						5780	3.40	...	−1.02	13
HD 140283	7.2	0.38	0.03	0.28	5,14	5600	...	...	−2.60	16
						5483	3.30	...	−2.40	12
						5630	3.20	...	−2.78	13
						5650	...	...	−2.79	14
						5650	3.30	1.5	−2.25	3
						5740	...	...	−2.19	17
						5640	...	...	−2.50	20
						5650	...	...	−2.60	15
						5570	3.30	1.5	−2.61	8
						...	...	...	−2.49	10
						5690	3.60	0.5	−2.57	19
						5640	3.10	1.5	−2.75	18
HD 160617	8.7	0.35	0.05	0.33	5	5861	3.50	...	−1.60	21
						5920	3.30	...	−1.74	13
						...	...	...	−1.84	10
						5910	3.50	1.5	−2.04	18
HD 161770	9.7	0.49	0.04	0.30	5	...	...	...	−1.38	10
HD 163810	9.6	0.42	0.10	0.26	14	5377	...	...	−1.55	14
						...	...	...	−1.40	10
HD 165195	7.3	0.92	0.14	0.70	1	...	...	...	−2.10	1
						4525	0.80	...	−1.80	22
						4500	1.50	2.8	−2.21	3
						4500	1.20	2.0	−2.21	4
						4475	...	...	−2.25	2
						4510	1.25	2.0	−2.22	19
HD 171496	8.5	0.76	0.15	0.41	1	...	...	...	−2.10	1
						4580	...	...	−1.75	2
HD 175305	7.2	0.50	0.16	0.31	1	...	...	...	−1.50	1
						5160	3.00	2.0	−1.53	4
						5150	...	...	−2.26	17
HD 186478	9.2	0.69	0.08	0.49	1	...	...	...	−2.60	1

TABLE 1—*Continued*

Star	V	b−y	m_1	c_1	ref	T_{eff}	log g	v_{turb}	[Fe/H]	ref
HD 187111	7.7	0.84	0.22	0.55	1	...	...	...	−2.10	1
						4300	0.75	...	−2.35	23
						4300	0.75	1.5	−2.35	4
						4260	0.50	1.4	−1.74	19
HD 189558	7.7	0.39	0.11	0.28	24	5660	4.00	...	−1.30	12
HD 190287	8.5	0.50	0.14	0.28	1	...	...	...	−1.50	1
HD 201889	8.1	0.39	0.14	0.28	5	5570	...	...	−1.40	15
						5580	...	...	−1.10	20
HD 204543	8.3	0.64	0.16	0.52	1	...	...	...	−1.60	1
						4750	1.15	2.9	−1.63	6
						4640	1.20	2.0	−1.79	8
						4710	...	...	−1.85	2
HD 211998	5.3	0.45	0.11	0.25	5	5200	3.50	...	−1.50	12
						...	...	...	−1.51	10
						5200	3.70	...	−1.54	13
						5120	3.50	1.0	−1.68	4
HD 216143	7.8	0.69	0.16	0.55	1	...	...	...	−2.30	1
						4500	1.10	3.0	−2.27	6
						4560	2.00	...	−2.23	23
						4520	1.60	1.5	−2.20	4
						4500	1.00	1.8	−2.11	8
						4565	...	...	−2.20	2
HD 218502	8.3	0.32	0.07	0.35	7	6000	3.80	1.5	−1.75	7
HD 218857	8.9	0.50	0.09	0.31	1	...	...	...	−2.10	1
						5200	2.00	2.5	−2.11	6
HD 221170	7.7	0.75	0.14	0.54	1	...	...	...	−2.60	1
						4350	0.00	...	−1.90	22
						4625	1.40	2.8	−2.04	3
						4500	1.30	1.4	−1.96	4
						4525	...	...	−2.20	2
HDE 232078		1.45	0.39	0.61	1	4000	0.40	...	−1.40	22
−30°1121	10.3	0.51	0.10	0.35	1	...	...	...	−2.00	1
−24°1782	9.9	0.47	0.04	0.29	5, 1	...	...	...	−2.70	1
						5250	2.60	1.8	−2.31	7
						5360	3.00	1.2	−2.35	8
						...	...	...	−2.56	10
−18°5550	9.3	0.69	-0.05	0.40	1	...	...	...	−3.50	1
						4750	0.80	2.9	−2.65	7
						4582	1.00	...	−3.00	25
						4600	1.30	3.0	−2.93	3
						4580	1.10	2.0	−2.99	8
						4750	1.10	2.5	−2.90	9
−14°5890	10.2	0.55	0.09	0.36	1	...	...	...	−2.10	1
						4905	...	...	−2.30	2
−10°0388	9.2	0.33	0.05	0.36	5	5860	3.30	...	−2.40	25
						5950	...	...	−2.20	20
						5980	3.50	...	−2.50	13
						5955	...	...	−2.71	11
						6010	3.20	1.5	−2.66	18
−10°0548	10.4	0.51	0.13	0.34	1	...	...	...	−1.60	1
−01°1792	9.2	0.51	0.23	0.27	5	5000	...	...	−1.02	16
						5000	...	...	−1.02	14
−01°2582	9.7	0.49	0.10	0.20	1	...	...	...	−1.90	1
						5000	1.20	1.8	−2.19	7
						5035	...	...	−2.30	2
+03°0740	9.8	0.31	0.07	0.35	5	6240	...	...	−2.90	11
						6110	...	...	< −2.30	20
						6110	3.20	1.5	−2.98	18
+04°2466	10.5	0.53	0.17	0.22	1	...	...	...	−1.40	1
						5010	...	...	−2.40	2

TABLE 1—*Continued*

Star	V	b−y	m_1	c_1	ref	T_{eff}	log g	v_{turb}	[Fe/H]	ref
+04°2621	10.0	0.62	0.06	0.47	1	...	...	...	−2.80	1
						4750	1.10	2.0	−2.21	7
						4725	...	...	−2.60	2
+06°0648	9.1	0.86	0.19	0.60	1	...	...	...	−2.30	1
						4500	0.80	2.4	−1.94	7
						4145	...	...	−2.25	2
+08°2856	10.1	0.69	0.13	0.62	1	...	...	...	−2.50	1
						4565	...	...	−2.25	2
+09°2870	9.4	0.64	0.12	0.49	1	...	...	...	−2.40	1
						4640	...	...	−2.50	2
+10°2495	9.7	0.50	0.09	0.35	1	...	...	...	−2.30	1
						4940	...	...	−2.15	2
+12°2547	9.9	0.63	0.14	0.42	1	...	...	...	−2.30	1
+18°2890	9.8	0.50	0.12	0.36	1	...	...	...	−2.00	1
+20°3603	9.9	0.32	0.05	0.31	5,14	6040	...	...	−2.30	15
						6000	...	...	−2.28	16
						6198	...	...	−2.26	14
						6000	4.00	...	−2.20	12
						6200	4.50	...	−2.49	13
+23°3912	8.9	0.37	0.08	0.29	5	5600	4.00	...	−1.70	12
						5600	...	...	−1.70	15
						5720	...	...	−1.30	20
						...	...	...	−1.29	10
+26°2606	9.7	0.34	0.05	0.28	5,14	5980	...	...	< −2.20	20
						5950	...	...	−2.89	11
+26°3578	9.4	0.31	0.05	0.37	5,14	5830	...	...	−2.60	15
						5800	...	...	−2.62	16
						6177	...	...	−2.51	14
						6000	3.25	...	−2.20	12
						6140	3.50	...	−2.57	13
+30°2611	9.2	0.82	0.33	0.55	1	...	...	...	−1.70	1
						4400	1.80	...	−1.70	22
						4400	0.90	1.7	−1.20	7
						4260	...	...	−1.55	2
+37°1458	8.9	0.44	0.07	0.22	5,14	5296	...	...	−2.39	14
						5420	...	...	−2.43	17
+58°1218	10.0	0.51	0.03	0.36	1	...	...	...	−2.80	1
						5000	1.10	2.2	−2.71	7
						5000	2.20	1.8	−2.46	3
						4980	...	...	−2.55	2
+72°0094	10.2	0.31	0.09	0.26	22	6160	...	...	−1.80	20
G5–36	10.8	0.40	0.07	0.28	5	...	...	...	−1.19	10
G18–54	10.7	0.37	0.08	0.28	5	...	...	...	−1.34	10
G20–08	9.9	0.36	0.05	0.25	5,14	5849	...	...	−2.59	14
						...	...	...	−2.03	10
G20–15	10.6	0.45	0.03	0.27	5,14	5657	...	...	−2.00	14
						6020	...	...	−1.56	17
						...	...	...	−1.58	10
G21–22	10.7	0.38	0.07	0.27	5,14	...	...	...	−1.23	10
G24–03	10.5	0.36	0.06	0.27	5,14	5866	...	...	−1.78	14
						...	...	...	−1.70	10
G30–52	8.6	0.50	0.25	0.27	14	4757	...	...	−2.12	14
						4880	...	...	−2.14	17
G33–09	10.6	0.41	0.10	0.28	5	5575	...	...	−1.48	14
G59–18	10.2	0.47	0.16	0.26	5	...	...	...	−1.08	10
G60–26	9.8	0.43	0.14	0.24	5	...	...	...	−1.15	10
G66–22	10.5	0.46	0.16	0.28	14	5060	...	...	−1.77	17
						...	...	...	−1.04	10
G90–03	10.4	0.37	0.04	0.29	5	...	...	...	−2.01	10
G102–47	10.3	0.46	0.10	0.23	5,14	5220	...	...	−2.25	17
						...	...	...	−1.62	10

TABLE 1—*Continued*

Star	V	b−y	m_1	c_1	ref	T_{eff}	log g	v_{turb}	[Fe/H]	ref
G122–57	8.4	0.53	0.27	0.31	14	4744	...	...	−1.71	14
G141–19	10.6	0.50	0.01	0.26	5	5155	...	...	−2.91	14
						5680	...	...	−1.80	17
						...	...	...	−1.95	10
G141–47	10.5	0.39	0.09	0.29	14	6056	...	...	−1.57	14
G170–47	8.9	0.45	0.06	0.28	14	5126	...	...	−2.91	14
G186–26	10.8	0.31	0.04	0.34	5	6220	...	...	−2.90	26
						6222	...	...	< −2.80	14
G205–42	10.0	0.43	0.10	0.23	14	5301	...	...	−2.18	14
G217–08	10.5	0.35	0.06	0.28	14	6066	...	...	−2.29	...
G243–63	7.7	0.48	0.13	0.30	14	...	...	...	−1.66	10
LP 608–62[a]	10.5	0.30	0.07	0.35	14	6250	...	...	−2.70	15

[a] Star LP 608-62 is also known as BD +1°2341p.

REFERENCES.—(1) Bond 1980; (2) Kraft et al. 1982; (3) Gilroy et al. 1988; (4) Gratton & Sneden 1987; (5) Schuster & Nissen 1988; (6) Luck & Bond 1981; (7) Luck & Bond 1985; (8) Gratton & Sneden 1988; (9) Peterson, Kurucz, & Carney 1990; (10) Schuster & Nissen 1989b; (11) Hobbs & Thorburn 1991; (12) Spite et al. 1984; (13) Magain 1987; (14) LCL, or Laird 1990; (15) Hobbs & Duncan 1987; (16) Peterson 1981; (17) Carbon et al. 1987; (18) Magain 1989; (19) Gratton & Sneden 1991; (20) RMB; (21) Spite & Spite 1986; (22) Leep & Wallerstein 1981; (23) Gratton & Ortolani 1986; (24) Olsen 1983; (25) Barbuy, Spite, & Spite 1985; (26) Hobbs et al. 1991.

lines were used to determine the rest velocity to confirm the identification of the Li I feature. In spectra with only the Li I feature, the measured wavelength was compared to the known radial velocity of the star to confirm the identification.

Equivalent widths were measured for the Fe I, Ca I, and Li I features, using the single-order spectrum reduction program of Fitzpatrick & Sneden (1987). Generally we used Gaussian approximations to the line profiles, with independent fits to the red and blue halves of the profiles. For a few distorted line profiles we supplemented or substituted direct profile integrations based on Simpson's Rule. For spectra in which the Li I line was not detected, an upper limiting equivalent width was estimated from the noise level in the nearby continuum. The equivalent widths for all features are given in Table 2.

We have compared our equivalent widths with those of three other major surveys of lithium in halo stars: RMB, Hobbs & Duncan (1987), and Spite et al. (1984). A plot of this comparison is given in Figure 4. The agreement is reasonably good; the mean of the difference between this study and others' measurements is 2.2 ± 2.2 mÅ, in the sense that our measurements are slightly higher. The scatter of an individual measurement from the mean is 9.7 mÅ. We call the reader's attention to an apparent trend of larger equivalent widths from our spectra for lines with EW > 80 mÅ, but we have too few points here to make a meaningful comparison, and most of our lines have equivalent widths substantially smaller than this value.

4. DERIVATION OF STELLAR METALLICITIES

In order to identify those subgiants with metallicities [Fe/H] ≤ −1.4, we determined Fe and Ca abundances for the program stars. Our analysis provides an independent and internally consistent estimate of metallicities near this boundary instead of relying on a heterogeneous set of metallicity estimates from the literature. Also, a substantial fraction of our sample has never been studied at high spectral resolution. A

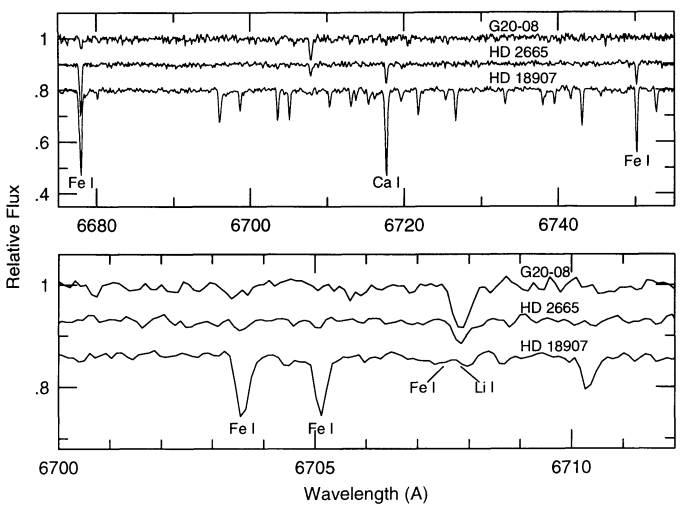

FIG. 3.—Spectra of three typical program stars. The lower part shows the detail of the region near 6707 Å. The atomic lines used in our analysis are indicated in the figure.

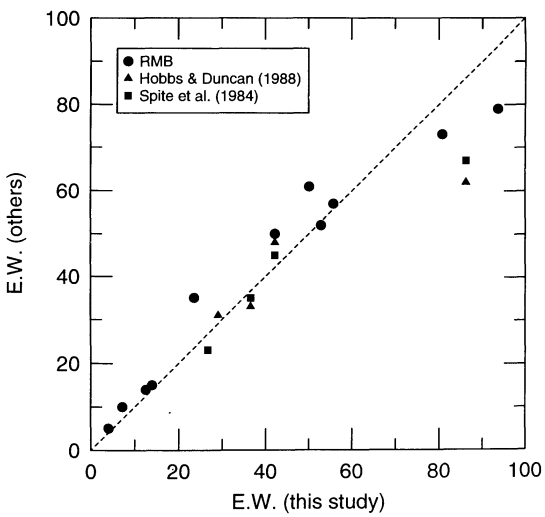

FIG. 4.—Equivalent widths for Fe I, Ca I, and Li I lines in common between this study and three papers from the literature. Refer to the inset in the figure for the identification of the symbols.

TABLE 2

EQUIVALENT WIDTHS

Star	6678Å Fe I	6703Å Fe I	6705Å Fe I	6707Å Li I	6717Å Ca I	6750Å Fe I
HD 97	105.1	18.9	15.1	12.1	71.3	52.5
HD 2665	68.1	7.3	...	15.0	24.9	22.6
HD 4306	21.6	...	...	17.7	7.7	...
HD 4906	113.5	29.3	30.7	9:	108.7	70.8
HD 5426	53.2	...	...	9.1	21.8	13.7
HD 6755	84.5	7.3	6.3	15.3	46.8	34.5
HD 18907	129.1	36.8	33.5	...	121.0	74.6
HD 21581	88.7	7.1	6.2	17.3	53.6	41.5
HD 24289	...	...	...	45.0	...	...
HD 24616	121.9	38.4	31.3	...	112.0	75.7
HD 44007	90.9	10.7	...	18.7	60.6	46.1
HD 45282	74.3	7.1	4.1	9.9	47.2	34.1
HD 76932	74.4	6.7	12.0	26.7	64.7	...
HD 84937	...	...	...	20[1]	...	...
HD 87140	71.9	...	...	13.8	37.6	...
HD 88609	...	...	...	<2	...	...
HD 94028	44.1	9.9	7.4	36.6	29.1	...
HD 97916	52.4	...	...	<5	55.1	...
HD 101063	93.5	19.9	...	12.3	68.6	...
HD 107752	35.4	...	...	<4	13.1	...
HD 108317	34.3	...	...	<4	15.3	...
HD 111721	91.8	16.5	12.2	17.2	72.9	...
HD 115444	31.8	...	...	<3	8.6	...
HD 122563	51.8	...	...	<2	11.9	...
HD 126587	23.6	...	...	14.5	10.9	...
HD 128279	41.1	...	...	11.4	17.3	7.5
HD 132475	55.7	...	...	52.8	38.1	...
HD 134169	...	...	...	44[2]	...	...
HD 140283	12.5	...	...	42.2	...	...
HD 160617	...	...	...	42[3]	...	...
HD 161770	51.1	...	6.4	44.9	31.4	14.4
HD 163810	83.0	9.5	7.6	22.1	54.9	...
HD 165195	103.8	7.7	2.9	<2	35.9	...
HD 171496	138.8	47.4	38.0	<3	124.8	...
HD 175305	...	...	8.2	13.7	60.9	...
HD 186478	56.8	...	...	<4	21.7	...
HD 187111	136.4	35.1	13.8	<2	93.4	...
HD 189558	...	...	...	42[2]	...	...
HD 190287	86.6	9.6	11.7	15.0	63.1	...
HD 201889	93.6	16.3	16.8	<4	86.2	...
HD 204543	109.8	7.7	...	<3	54.5	52.3
HD 211998	...	...	...	13[2]	...	...
HD 216143	92.1	8.2	...	<8	30.3	40.1
HD 218502	20.0	...	...	30.0	10.0	...
HD 218857	61.6	...	...	12.1	...	21.3
HD 221170	94.0	8.6	...	<3	41.7	45.6
HDE 232078	198.1	67.4	23.5	32.8	136.5	143.0
−30°1121	74.1	...	7.5	14.6	30.5	28.8
−24°1782	16.0	...	...	12.6	10.4	...
−18°5550	28.6	...	...	16.8	...	...
−14°5890	58.9	...	...	25.8	28.6	...
−10°0388	7.2	...	...	23.6	...	...
−10°0548	85.1	17.1	...	17.2	57.0	...
−01°1792	112.4	30.0	25.0	10:	104.4	...
−01°2582	40.9	...	...	10.2	19.3	...
+03°0740	...	...	...	21[4]	...	...
+04°2466	52.9	...	...	<6	38.0	...
+04°2621	49.8	...	...	<5	17.4	...
+06°0648	...	13.5	8.1	<4	46.5	51.8
+08°2856	99.3	...	...	8:	42.8	...
+09°2870	70.4	...	...	<4	23.6	...
+10°2495	67.6	...	...	21.3	29.2	...
+12°2547	198.1	86.0	62.7	<4	180.7	...
+18°2890	88.0	12.0	8.6	<4	57.7	...
+20°3603	...	...	...	27[1]	...	...
+23°3912	50.1	...	...	80.8	41.2	13.9
+26°2606	...	...	...	35[4]	...	...
+26°3578	...	...	...	27[1]	...	...
+30°2611	166.1	52.4	25.1	<6	104.8	115.6
+37°1458	42.9	...	...	17.0	17.3	...
+58°1218	27.9	...	...	17.2	...	...
+72°0094	...	...	...	27[3]	...	..
G5-36	54.4	9.2	7.7	44.2	53.1	...
G18-54	52.3	...	...	34.9	...	...
G20-08	14.5	...	...	36.3	...	...
G20-15	40.7	...	...	28.3	36.9	...
G21-22	63.5	...	...	41.4	37.9	...
G24-03	38.4	...	...	28.5	21.4	...
G30-52	...	15.6	11.0	...	59.7	59.8
G33-09	...	...	7.7	35.2	55.9	30.5
G59-18	94.7	18.5	15.0	15.7	78.9	...
G60-26	81.8	7.6	11.0	13.6	64.6	...
G66-22	115.2	19.6	21.2	6:	86.8	...
G90-03	23.6	...	...	43.5	20.9	...
G102-47	71.5	...	...	17.5	44.4	25.2
G122-57	128.5	41.0	32.0	<3	120.8	...
G141-19	25.5	...	...	32.5	13.8	...
G141-47	59.9	9.6	7.8	35.0	39.8	...
G170-47	27.8	...	...	14:	7.5	...
G186-26	...	...	...	≤3[5]		...
G205-42	54.1	...	...	24.0	25.6	24.8
G217-08	15.4	...	...	32.6	...	...
G243-63	...	8.3	4.3	13.1	41.1	38.0
LP 608-62	...	...	...	23[1]	...	...

REFERENCES.—(1) Hobbs & Duncan 1987; (2) Spite et al. 1984; (3) Spite & Spite 1986; (4) RMB; (5) Hobbs et al. 1991.

further motivation for determining metal abundances was to ascertain the reliability of our model atmosphere and line analysis procedures by using those program stars with several previous spectroscopic studies.

The first step in determining abundances from the measured equivalent widths was to estimate the stellar parameters $T_{\rm eff}$, log g, microturbulent velocity v_t, and an approximate metallicity. These atmosphere parameters then were used as input to compute a grid of model stellar atmospheres using the MARCS computer code (e.g., Gustafsson et al. 1975), kindly made available to us by Michael M. Briley.

Most stars in our sample fall in the temperature range for which the Strömgren $b - y$ index is a reliable temperature indicator. Calibrations for $b - y$ are available from several authors (Magain 1987; Olsen 1984; Saxner & Hammerbäck 1985; Schuster & Nissen 1989a) for different regimes of $b - y$ and [Fe/H], but none of these was specifically suitable for our sample. We used the temperatures available from the literature for many of our well-studied and metal-poor stars for which reddening is known to be small (a total of 37 stars) to determine a new relation for $T_{\rm eff}$ vs. $b - y$ applicable to metal-poor stars within the range $0.3 < b - y < 0.5$. These stars provided the linear calibration

$$T_{\rm eff} = 7600. - 5200 * b - y \quad (1)$$

which reproduces well the temperatures available from the lit-

erature. For cooler stars in the range $0.5 < b - y < 0.65$ we adopted the calibration of Olsen (1984). A few of the stars are too cool for the $b - y$ color to provide a reliable temperature, but in these cases (generally the cooler and more well-studied giants) temperatures are available from the literature from previous analyses.

One difficulty in applying $b - y$ to estimate the effective temperature is its sensitivity to reddening. The subgiants are at moderate distances (typically 125 pc for a 9th mag star of absolute magnitude 3.5) and can be expected to be reddened. Reddening estimates are available from the literature (LCL or Bond 1980), or can be obtained from the Hβ photometry for many of the stars using the calibration of Crawford (1975). For others, reddening can be estimated from the maps of Burstein & Heiles (1982). For many of the stars, however, the uncertainty in the effective temperature can be a few hundred degrees based just on the uncertainty of our reddening estimate. Fortunately, many of the stars are unreddened, or virtually so.

In practice, more than half of the stars in our sample of subgiants have one or more spectroscopic or broad-band color temperature estimates in the literature. We compared in detail the temperatures derived from the $b - y$ temperature calibrations (both without reddening corrections and with reddening corrections when a reliable estimate of reddening is available) with other temperature determinations from the literature. Then final $T_{\rm eff}$ values for individual stars were adopted based on our estimates of the reliability of various sources. In almost all cases the temperature values quoted in literature sources, the $b - y$ temperature calibrations, and our final temperature estimates agreed to within 100 K. The few exceptions include HD 160617, for which we adopt a spectroscopic temperature (from several sources) of 5900 K while the $b - y$ color suggests 6200 K, and several of the red giants, such as HD 122563, BD +9°2870, BD −18°5550, and HD 204543, for which we adopt temperatures slightly hotter than might be expected from their $b - y$ colors. For G217−8 we adopt a temperature of 6050 K from the analysis of LCL, while the $b - y$ color would indicate a somewhat cooler temperature. For the coolest stars ($b - y > 0.65$) we relied on spectroscopic temperature taken from the literature. The effective temperature finally adopted for each star are included in Table 3.

We estimated the stellar gravities using the M92 color magnitude diagram, following Bond (1980) to derive an empirical relation between $T_{\rm eff}$ and log g, assuming a mass of 0.8 $M_\odot$ for the M92 subgiants. Initial metallicity estimates for all stars were taken from the literature and are listed in Table 1. The initial abundance derivation trials showed, however, that the abundances from Fe I, Ca I, and Li I features were very insensitive to the assumed model metallicities. As a result, models were computed only for metallicities of [Fe/H] = −1 and −2. Microturbulent velocities were initially assumed to increase fairly smoothly from 1.0 km s^{-1} for the hottest models ($T_{\rm eff}$ = 6000 K) to 2.0 km s^{-1} for the coolest (4300 K) models, from our assessment of the average values of this parameter reported in the literature. Minor adjustments, never more than ±0.5 km s^{-1}, were made for individual stars for which a compelling case could be made from our small line data set.

We then used the Fe I and Ca I lines listed in Table 2 to determine iron and calcium abundances in a uniform way for our sample. In Table 3 we list these abundances. Oscillator strengths for the Fe I λλ6677.99, 6703.57, and 6750.15 lines were taken from the critical compilation of Fuhr, Martin, & Wiese (1988). The λ6705.1 Fe I line apparently does not have a reliable laboratory oscillator strength. The *gf*-values for this line were derived from an inverted solar analysis using an equivalent width measured on the Liège solar atlas (Delbouille, Neven, & Roland 1973) and the Holweger & Müller (1974) solar model atmosphere. An extensive study of Ca I oscillator strengths published by Smith & Raggett (1981) includes the λ6717.69 feature. However, a companion analysis of the calcium abundance in the Sun and in Procyon by Smith (1981) reveals that this line yields an abundance clearly higher than the mean (especially in Procyon), emphasizing Smith's contention that this feature is "clearly blended in both wings." Results from the λ6717 line were treated with caution (see below).

Are our stellar metallicities reliable? We stress that our derivations of metallicity indicators from at most a few lines of two neutral species cannot possibly take the place of careful abundance analyses of many lines from different ionization stages of many elements. However, our task here is simply to ask whether our metallicity estimates are good enough to discover or confirm members of the true set of very metal-poor stars. We first address this question simply by correlating our Fe abundances with spectroscopic (high- and low-resolution) and photometric metallicity determinations from the literature. We include only literature data sets that contain a reasonably large sample of stars, in order to ascertain both mean offset and scatter between our determinations and the literature values. In Figure 5 the various correlations are displayed. Inspection of this figure suggests that on average our [Fe/H] abundances correlate well with the work of others, and the scatter of individual points is consistent with the expected uncertainties in this and other data sets. Moreover, linear least-squares fits through the correlations would not deviate significantly from the dashed lines that depict "perfect correlation" in most of the figure panels. Some brief exposition on the individual correlations is appropriate.

First consider high-resolution, high S/N data sets from the literature, depicted in Figure 5*a*. For this panel only, we have included abundances from more than one source, since the number of stars in common between this study and individual high-resolution studies is typically quite small. Only literature abundance sets derived from low-noise digital detectors were employed here. The literature data were taken from Magain (1987, 1989), François (1986, 1987, 1988), Gratton & Sneden (1987, 1988, 1991), and Gilroy et al. (1988). For stars included in more than one of these studies (e.g., HD 140283), we have used a straight mean of the published abundances. No systematic deviations between the present Fe metallicities and these various high-resolution results are seen. Writing the mean difference in this correlation and in others of Figure 5 as $\Delta \equiv \langle [{\rm Fe/H}]_{\rm others} - [{\rm Fe/H}]_{\rm this\ study} \rangle$, the comparison with high-resolution, high S/N studies yields $\Delta = -0.02 \pm 0.04$ for 19 stars, with the scatter of an individual point from the mean $\sigma = 0.19$. The comparison would improve markedly by the excision of just the wayward point for HD 187111, a cool and difficult-to-analyze giant; then $\Delta = +0.01 \pm 0.03$, with $\sigma = 0.13$.

In Figure 5*b*, our results are correlated with the high-resolution but low S/N data of LCL. Unsurprisingly, we find the scatter somewhat higher here, and there is a systematic offest with the LCL study deriving systematically lower abundances than we do: $\Delta = -0.35 \pm 0.06$ for 18 stars, with $\sigma = 0.25$. However, this correlation still gives reasonably

TABLE 3

MODELS AND ABUNDANCES

Star	T_{eff}	log ϵ(Li)	[Fe/H]	[Ca/H]	Star	T_{eff}	log ϵ(Li)	[Fe/H]	[Ca/H]
HD 97	5000	0.81	−1.23	−0.92	−30°1121	5100	0.99	−1.62	−1.58
HD 2665	5100	0.90	−1.89	−1.80	−24°1782	5300	1.13	−2.70	−2.10
HD 4306	4950	0.92	−2.87	−2.45	−18°5550	4600	0.42	−3.15	...
HD 4906	5100	0.77	−0.84	−0.18	−14°5890	4950	1.10	−2.07	−1.72
HD 5426	5100	0.77	−2.08	−1.83	−10°0388	5950	2.00	−2.52	...
HD 6755	5200	1.12	−1.52	−1.31	−10°0548	5100	1.07	−1.07	−0.98
HD 18907	5000	...	−0.78	+0.01	−01°1792	5000	0.78	−0.94	−0.28
HD 21581	4900	0.84	−1.73	−1.35	−01°2582	5100	0.83	−2.29	−1.89
HD 24289	5570	2.00	...	...	+03°0740	6110	2.07	...	...
HD 24616	5000	...	−0.78	−0.14	+04°2466	5000	< 0.50	−2.15	−1.47
HD 44007	4900	0.88	−1.50	−1.15	+04°2621	4550	−0.30	−2.83	−2.31
HD 45282	5400	1.12	−1.29	−1.09	+06°0648	4500	< −0.50	−1.91	−1.70
HD 76932	5900	2.02	−0.90	−0.56	+08°2856	4560	< 0.00	−2.05	−1.78
HD 84937	6252	2.10	...	...	+09°2870	4600	< −0.30	−2.48	−2.10
HD 87140	5000	0.86	−1.75	−1.58	+10°2495	5000	1.07	−1.83	−1.70
HD 88609	4510	< −0.80	...	...	+12°2547	4500	< −0.50	−0.72	+0.14
HD 94028	5800	2.09	−1.51	−1.28	+18°2890	5000	< 0.30	−1.61	−1.15
HD 97916	6000	< 1.30	−1.38	−1.23	+20°3603	6000	2.12	...	...
HD 101063	5000	0.81	−1.13	−0.90	+23°3912	5600	2.38	−1.59	−1.11
HD 107752	4700	< −0.10	−2.88	−2.33	+26°2606	5980	2.20	...	...
HD 108317	5300	< 0.60	−2.32	−1.91	+26°3578	6000	2.05	...	...
HD 111721	5000	0.97	−1.34	−0.89	+30°2611	4400	< −0.40	−1.35	−1.08
HD 115444	4800	< −0.10	−2.72	−2.47	+37°1458	5300	1.27	−1.97	−1.87
HD 122563	4600	< −0.60	−2.75	−2.45	+58°1218	5000	0.97	−2.66	...
HD 126587	4750	0.56	−3.06	−2.37	+72°0094	6160	2.22	...	...
HD 128279	5100	0.88	−2.32	−1.99	G5–36	5600	2.03	−1.35	−0.82
HD 132475	5500	2.04	−1.48	−1.23	G18–54	5800	2.07	−1.33	...
HD 134169	5800	2.18	...	...	G20–08	5850	2.13	−2.26	...
HD 140283	5650	2.05	−2.52	...	G20–15	5600	1.80	−1.78	−1.22
HD 160617	5900	2.23	...	...	G21–22	5700	2.08	−1.09	−1.03
HD 161770	5050	1.50	−2.12	−1.64	G24–03	5800	1.97	−1.63	−1.42
HD 163810	5400	1.51	−1.23	−1.00	G30–52	5000	...	−1.31	−1.14
HD 165195	4490	< −0.80	−2.26	−1.97	G33–09	5500	1.82	−1.27	−0.94
HD 171496	4500	< −0.60	−1.12	−0.35	G59–18	5200	1.13	−1.08	−0.65
HD 175305	5190	1.08	−1.50	−1.00	G60–26	5400	1.26	−1.22	−0.83
HD 186478	4600	< −0.10	−2.68	−2.15	G66–22	5300	0.79	−0.90	−0.65
HD 187111	4300	< −1.20	−1.76	−1.22	G90–03	5900	2.25	−1.93	−1.41
HD 189558	5600	2.00	−1.30	...	G102–47	5200	1.18	−1.69	−1.30
HD 190287	5100	1.01	−1.38	−1.01	G122–57	4800	< −0.10	−0.92	−0.13
HD 201889	5600	0.91	−0.73	−0.22	G141–19	5150	1.43	−2.59	−2.01
HD 204543	4650	< −0.40	−1.96	−1.57	G141–47	6000	2.23	−1.13	−0.98
HD 211998	5210	1.04	...	...	G170–47	5250	1.13	−2.42	−2.30
HD 216143	4500	< −0.10	−2.18	−2.05	G186–26	6220	< 1.28	...	...
HD 218502	6000	2.16	−1.96	−1.77	G205–42	5300	1.44	−1.51	−1.61
HD 218857	5100	0.91	−1.87	...	G217–08	6050	2.24	−2.05	...
HD 221170	4625	< −0.10	−1.96	−1.74	G243–63	5200	1.05	−1.39	−1.36
HDE 232078	3950	−0.22	−-1.73	−1.31	LP 608–62	6250	2.21	...	...

strong strong support to LCL's contention that their low S/N spectra can yield very reliable abundances, at least in a statistical sense.

As discussed above, Strömgren photometry has proved to yield sensitve metallicity discriminants for Population II stars, so in Figure 5*c* we have correlated our abundances with the Fe values deduced by Schuster & Nissen (1986b) from their Δm_1 indices for warm Population II stars (dwarfs and subgiants), and in Figure 5*d* a similar correlation is shown for the Bond (1980) sample of cool Population II stars (subgiants and giants). The correlation with the Schuster & Nissen data is reasonably tight if we exclude a couple of stars for which they derive much higher abundances than we do: $\Delta = +0.08 \pm 0.03$ for 22 stars, with $\sigma = 0.16$. For the giants the relationship between our data and Bond's ($\Delta = -0.12 \pm 0.05$ for 33 stars, excluding two outlying points) shows more scatter: $\sigma = 0.27$. We suspect that this increased scatter simply relects the increased difficulty in applying *uvby* photometry to cool giant stars.

Finally, in panels Figures 5*c* and 5*f* we show the correlations with the abundances deduced from low-resolution scanner data by the Lick group. The data for giants (Kraft et al. 1982) and for dwarfs (Carbon et al. 1987) are split because their [Fe/H] values were determined in fundamentally different ways. For giants, their abundances were based on calibrations of their observations of the Ca II H and K line strengths, and the correlation between their abundances and ours are quite satisfactory: $\Delta = -0.09 \pm 0.05$ for 23 stars, with $\sigma = 0.22$. The scatter would be reduced further if we allowed for the apparent small systematic drift in the correlation with metallicity, but in

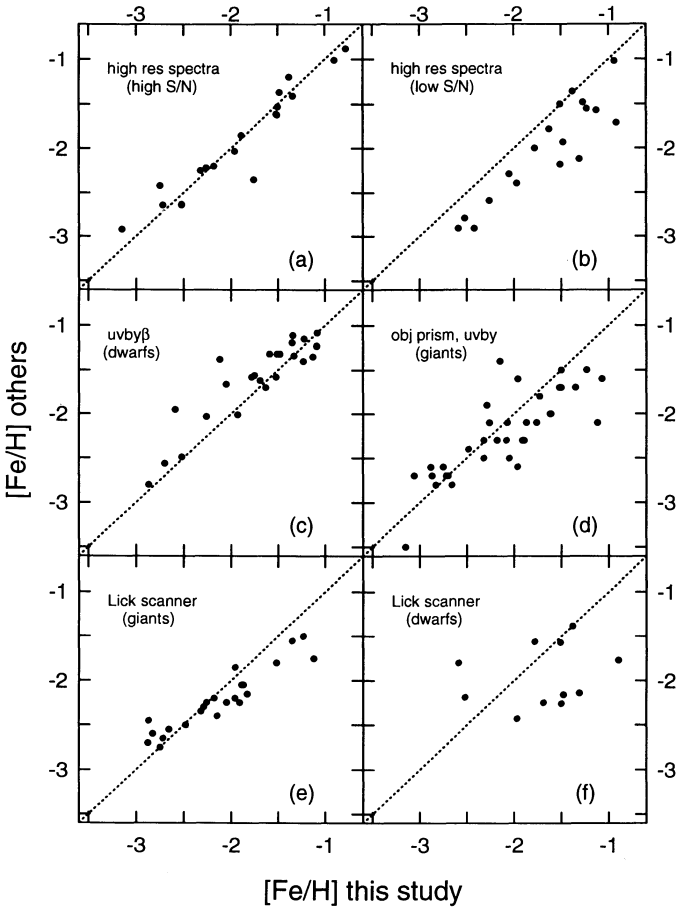

FIG. 5.—Comparisons of the [Fe/H] values derived from our spectra with those quoted in literature surveys. The slanting dashed lines in each panel signify perfect agreement between the abundance estimates. See the text for descriptions of the data sets consulted for these comparisons.

any case the H and K indices clearly are measuring the same things as do our [Fe/H] values. The Lick scanner abundances for dwarfs were derived from a combination of $\delta(U-B)$ values from the literature and their own synthetic spectrum calculations. Here the correlation with our data is disappointing, but the Carbon et al. paper warns that their [Fe/H] values probably have uncertainties of scatter at least as large as ± 0.3 dex, so the size of the scatter here is not surprising.

Taken as a whole, the various literature data sets allow us to identify stars for which our abundances may have greater uncertainties. In this spirit, we alert the reader that our [Fe/H] values for three of the over 90 stars in our program differ significantly from other, published estimates. Our metallicity for HD 161770 is some 0.8 dex lower than that derived by Schuster & Nissen (1989b), our value for HD 171496 is about 0.8 dex higher than suggested by Bond (1980) and by Kraft et al. (1982), and our value for G30−52 is 0.8 dex higher than derived by both LCL and Carbon et al. (1987). Our results for these stars should be viewed with special caution. More mild cases of disagreement between our [Fe/H] values and literature are not discussed here, but may be deduced by comparison of the data of Tables 3 and 1.

A second test of our metallicity estimates lies in the correlation of our [Ca/H] and [Fe/H] values. This correlation, displayed in Figure 6, suggests that for stars with [Fe/H] < -1, $\langle$[Ca/Fe]$\rangle = +0.33 \pm 0.02$ for 62 stars. This relative overabundance of Ca in metal-poor stars is qualitatively in agreement with the results of more extensive studies of this element (see several of the high-resolution abundance surveys cited above, or review articles such as that of Wheeler, Sneden, & Truran 1989). The agreement is reasonable also quantitatively, remembering that our assumed solar Fe abundance, log $\epsilon = 7.52$, is about 0.1 dex lower than assumed in many earlier analyses. The scatter of individual points in Figure 6 ($\sigma = 0.18$) serves as a good estimate of the uncertainty for individual abundance determinations from species with but a single line present (Ca, and the Li to be discussed next). Finally, for the few stars with [Fe/H] > -1, the Ca overabundance apparently increases, instead of declining toward [Ca/Fe] $\simeq$ at [Fe/H] $\simeq 0$. We regard this not as a real abundance trend but rather as a manifestation of the effect pointed out by Smith (1981) that there are weak blends in the wings of the λ6717 Ca I line. These blends effectively disappear in line-weak stars that comprise most of our sample.

5. DETERMINATION OF THE LITHIUM ABUNDANCES

In the case of our subgiants, the derived lithium abundance is a strong function of the adopted effective temperature, a slight function of the adopted microturbulent velocity and the stellar metallicity, and virtually independent of the assumed surface gravity. Since the lithium feature is weak (less than 50 mÅ in all but one case), the sensitivity to microturbulence is limited. The high thermal velocity of the relatively lightweight lithium atoms in the stellar photosphere is also a more significant factor in broadening the line than is the microturbulence. An accurate estimate of the stellar effective temperature is the most important parameter.

Since the lithium determination is not a strong function of gravity, microturbulence, or metal abundance, we computed a series of curves of growth at temperatures from 4500 to 6000 K, in 500 K steps, at a metallicity of [Fe/H] $= -2.0$, a surface gravity of log $g = 3.0$, and a microturbulence of 1.5 km s^{-1}. The models used to calculate the curves of growth were produced as described above. The curves of growth were calcu-

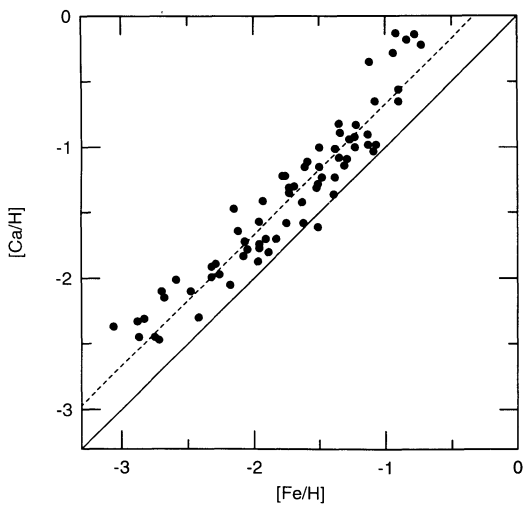

FIG. 6.—The correlation between our Fe and Ca abundances. The solid slanting line defines the position of [Ca/Fe] = 0.00, and the dashed line is set at [Ca/Fe] = +0.33, the derived mean Ca overabundance from stars with [Fe/H] < -1.

lated using the detailed structure of the lithium feature and integrating the equivalent width from a synthetic spectrum. Atomic line data for the lithium feature were obtained from Andersen et al. (1984).

We interpolated between curves to the temperature appropriate for an individual star to obtain the lithium abundance from the measured equivalent width. For a few stars in Table 3, we have adopted lithium equivalent widths and metallicities from the literature, but have redetermined temperatures and derived lithium abundances as for our own data. These stars are noted in Table 3. For these stars, no Ca or Fe abundances are given because we did not redetermine abundances for either of these species.

A similar analysis procedure was used to estimate the uncertainty in our lithium abundances from measurement uncertainties and uncertainties in reddening and temperature. The estimated uncertainty in the lithium abundance for each star is dominated by the uncertainty in temperature. For stars which have been studied extensively, providing spectroscopic estimates of the effective temperature, and for warmer stars with little or no reddening, the adopted temperatures are probably within 100 K of the true temperature. For these stars we estimate the uncertainty in our lithium abundances to be 0.15 dex. For stars with more or uncertain reddening and without previous spectroscopic determinations, temperatures are more uncertain and could be higher than we estimate. A higher adopted temperature would yield a lithium abundance higher by about 0.1 dex per 100 K. The lithium abundances would then be higher than we present in Table 3.

For HDE 232078, we adopted a temperature of 4000 K based on the analysis of Leep & Wallerstein (1981), but note that the reddening is large and uncertain for this star. Our measured equivalent width of 32 mÅ suggests a lithium abundance of log ϵ(Li) = -0.2 at this temperature, but the value is uncertain because of the uncertainty in the reddening and temperature. The lithium abundance HDE 232078 is of similar value to the upper limits in other, warmer red giants; lithium is detectable in this case because the star's cool temperature increases the strength of the lithium feature. Because the metallicity of HDE 232078 is near our cutoff of [Fe/H] < -1.4, and because the metallicity is also uncertain due to the reddening, we will not include this star in further discussion.

Our Li abundances are in excellent agreement with those published in other surveys. We have two to five stars in common with those in the studies of Spite et al. (1984), Hobbs & Duncan (1987), RMB, and Hobbs & Thorburn (1991). The mean differences between our Li abundance and the ones in these cited papers typically is $\simeq 0.05$ dex, and for no star is the difference as great as 0.2 dex.

6. LITHIUM DILUTION IN HALO SUBGIANTS

The process of lithium dilution in subgiants can be examined quantitatively by using effective temperature as a parameter to indicate evolutionary phase from the main-sequence turnoff to the base of the red giant branch. We have plotted log ϵ(Li) versus $T_{\rm eff}$ in Figure 7 for the stars in Table 3, using different symbols for stars in three metallicity ranges: [Fe/H] > -1.4, $-1.4 \geq$ [Fe/H] > -1.9, and $-1.9 \geq$ [Fe/H]. Figure 7 confirms the expected onset of convective dilution at a temperature near 5600 K, and the decline in the surface lithium abundance at cooler temperatures. Note that the main-sequence turnoff for halo subdwarfs occurs at a temperature of about 6200 K. We confirm that the spread in lithium abundance for subgiants near 6000 K is small and that the mean value is near log ϵ(Li) = 2.1. The regime near 5500 K (the classical Hertzsprung gap) is poorly sampled because of the rapid pace of stellar evolution at this temperature. The dependence of the lithium abundance on temperature does not differ significantly among the three groups of stars in different metallicity ranges.

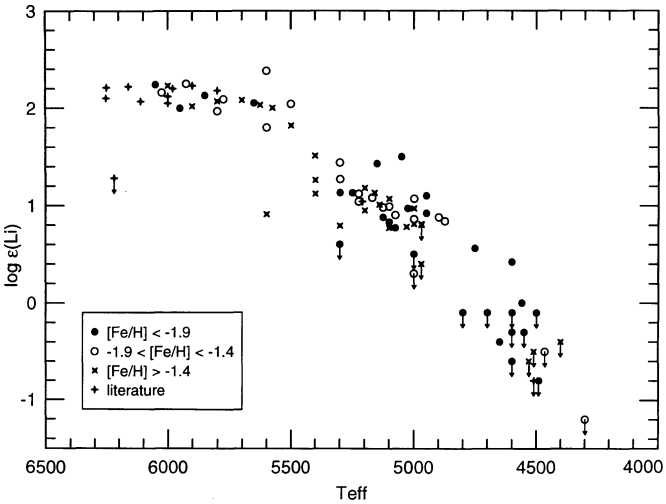

FIG. 7.—Lithium abundances plotted against stellar effective temperatures for all of the program stars. Different symbols have been employed to separate the stars into the three metallicity regimes indicated in the inset.

Lithium abundance is again plotted versus effective temperature in Figure 8, in which we include only stars with [Fe/H] < -1.4. At a temperature of about 5000 K lithium *dilution* is complete corresponding roughly to the deepest extent of the convective envelope. The "typical" dilution factor is only about 16, but, in contrast to the spread in lithium abundance in the warmer subgiants in the predilution phase, the range in the lithium abundance is a factor of 10 or more. At even cooler temperatures characteristic of stars on the red giant branch and on the asymptotic giant branch, we see upper

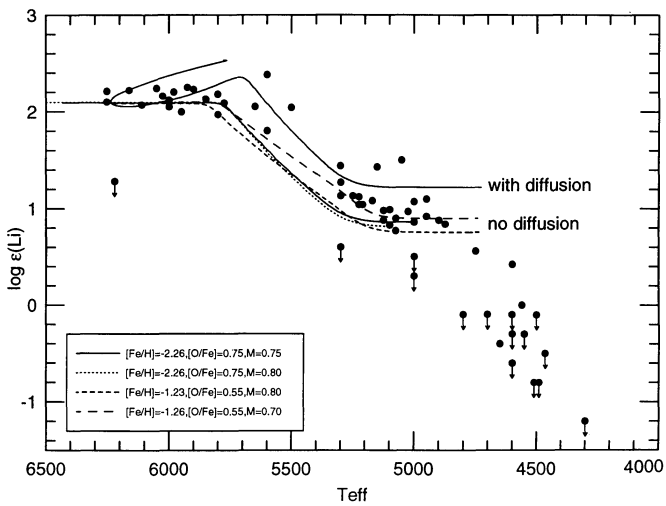

FIG. 8.—Another lithium abundances versus effective temperature plot, this time restricting the observed sample to stars for which we have derived [Fe/H] < -1.4. Lines representing several theoretical predictions (Proffitt & Michaud 1991) for lithium dilution as a function of effective temperature have been added to this figure.

limits to the lithium abundance at substantially lower lithium abundances, factors of 100 or more below the surface abundance at the end of the main-sequence lifetime.

Several investigators have recently examined the effects of stellar evolution on the surface lithium abundances in metal-poor stars. Pinnsoneault, Deliyannis, & Demarque (1991), Deliyannis et al. (1990), and Proffitt & Michaud (1990) have considered the effects of rotation and diffusion on the abundance of lithium in subdwarfs near the turnoff and on the lower main sequence. Proffitt & Michaud have further considered the effects of dilution as metal-poor stars evolve from the turnoff to the base of the giant branch.

The lithium abundances in subdwarfs can be compared directly to theoretical predictions by Proffitt & Michaud (1990) plotted in Figure 8. The models are selected with initial masses of 0.7–0.8 $M_{\odot}$, and with compositions from [Fe/H] = −1.23 to −2.26. We include four models computed without diffusion and one in which diffusion is included. The surface lithium abundance in the models has been adjusted to be log ϵ(Li) = 2.1 at the main-sequence turnoff. For the model with diffusion, this requires that the initial lithium abundance in the model be log ϵ(Li) = 2.5. In the model with diffusion, lithium settles below the surface, reducing the surface abundance, but does not fall far enough to reach a temperature where it will be burned. Lithium is effectively stored in a lithium-rich layer just below the surface. When surface convection begins, the lithium-rich layer is mixed to the surface, initially raising the surface lithium abundance. The lithium abundance at even cooler temperatures falls as expected as convection continues to deepen into the star. Once the convective zone reaches its deepest extent, the dilution is complete, and the lithium abundance should level off at a constant value.

In the broadest sense our observations provide strong support to the theoretical models. Convective dilution begins at approximately the temperature predicted, and the convective envelope reaches its greatest extent, as shown by the "plateau" in Figure 8, at a temperature predicted by models. The extent of dilution, given roughly by the ratio of the greatest depth of the convective zone to the depth of the lithium surface layer at the end of the main-sequence lifetime, compares quantitatively to observations of lithium in stars near 5000 K. Detailed comparison between the theory and the observations, however, raises several questions which must be examined.

1. *Do the subgiants provide evidence that diffusion of lithium occurs in halo main-sequence stars?*

Evidence that diffusion may have affected the surface abundances of lithium in halo stars at the main-sequence turnoff can be found in the relatively high abundance of lithium in stars near 5600 K, and also in the slightly higher abundance of lithium in the plateau stars compared to the nondiffusion models.

The high lithium abundances found in the four stars near a temperature of 5600 K may offer evidence for a "diffusion bump" as the newly formed convective envelope mixes up lithium stored below the surface. Because of the potential impact of this conclusion, we must examine in some detail whether these four stars are, in fact, subgiants. The abundance of lithium in BD +23°3912 is the highest in our sample. This star has been considered to be a dwarf (cf. RMB, who confirm our high lithium abundance), but the Strömgren colors are more consistent with its identification as a subgiant. No parallax is available. The case for HD 140283 was discussed earlier, and we feel confident in its assignment as a subgiant. As also discussed earlier, the evolutionary status of HD 132475 is ambiguous. The parallax suggests the star is a subdwarf while, like HD 140283, both the Strömgren photometry and spectroscopic analyses suggest it must be a subgiant. The lower lithium abundance found in G20−15 is more consistent with nondiffusion models.

At the end of the dilution phase (at about $T_{\rm eff}$ = 5000) the lithium is observed to level off at an abundance of log ϵ(Li) = 0.9, giving a dilution factor of about 16. The level of this observed lithium plateau abundance is higher than one would expect from the nondiffusion models. Only a modest increase, however, in the main-sequence lithium skin depth would bring the postdilution lithium abundances in the models into agreement with the observations.

We conclude that observations raise a mild possibility that diffusion of lithium may be at work in the main-sequence phases of metal-poor stars, but support for this idea is not definitive. We do note, however, that Deliyannis & Demarque (1991) argue that the diffusion models are not a good fit to the lithium versus temperature relation for the subdwarfs.

2. *What causes the large apparent spread in lithium abundance at the end of the dilution phase?*

The spread in the lithium abundance in the immediate postdilution phase (i.e., at a temperature of about 5000 K) is about an order of magnitude, but the spread in lithium abundance in the predilution phase is quite small (with the exception of star G186−26 of Hobbs et al. 1991). Our sample of subgiants at the dilution plateau contains a few stars with lithium abundances substantially higher than the mean, as well as stars with lower lithium abundances.

The two lithium-rich subgiants, HD 161770 and G141−19, are both extremely metal poor stars. The stars are sufficiently cool that they are unlikely to be subdwarfs misidentified as subgiants. Examination of Figure 4 of RMB further suggests that subdwarfs at this temperature have much lower lithium abundances, near log ϵ(Li) = −0.6. The reddening is uncertain for both stars, and both could have hotter temperatures than we adopt. Raising the temperature, however, will also raise the derived lithium abundance, and cannot explain why the lithium abundances are so high.

The stars with unusually low lithium abundances in this temperature regime include HD 108317, BD +4°2466, and BD +18°2890. The low lithium abundances in these stars are similar to what is seen by RMB at similar temperatures among the subdwarfs. BD +4°2466 (as well as BD −1°2582, with a more typical lithium abundance) is a CH-strong star from Bond (1980). Bond argues that the strong CH depresses c_1, and that both stars are giants. HD 108317 and BD +18°2890 both have c_1 indices consistent with being subgiants, but parallax data are not available. Bond lists both of these as giants, and spectroscopic surface gravities are in the range appropriate for subgiants or giants (Cayrel de Strobel et al. 1992).

The most likely explanation for the spread in the lithium abundance observed in the postdilution phase is that it results from differences in the lithium skin depth at the end of main-sequence evolution or differences in the extent of diffusion of lithium into the star.

3. *What causes the very low lithium abundances observed in halo red giants?*

All of the metal-poor red giants in our sample have very low lithium abundances [i.e., log ϵ(Li) < 0.0]. These stars are the well-known halo red giants studied by Bond (1980) and

analyzed by a variety of investigators, as listed in Table 1. The very low lithium abundances in the red giants suggest some lithium destruction mechanism, not just dilution, must act to reduce the lithium abundance after the convective envelope reaches its deepest extent into the star. Since these are all quite metal-poor halo stars ([Fe/H] < -1.7) they are evolved from stars very similar in mass to the subdwarfs at the main-sequence turnoff, and we cannot invoke main-sequence depletion to explain the very low lithium abundances. Some mechanism to burn lithium on the giant branch is necessary to explain these low lithium abundances. Either the bottom of the convection zone is hot enough to burn lithium or some mixing process below the convection zone transports envelope material to greater depth and back out. Note that the lithium abundance is already quite low even in the lower luminosity giants in our sample of red giants, but that we do detect lithium in a few higher luminosity giants.

The spread in the lithium abundance among the red giants may be as much as two orders of magnitude, but it is difficult to estimate given the uncertainty of our upper limits. The spread in the lithium abundances in the red giants may result simply from the wide spread in the immediate postdilution phase, or the process by which lithium is depleted in red giants may act with different efficiency in different stars.

Finally, it is worth noting that the apparent problem of "too much processing" that we see in our lithium data is shared by other light elements in metal-poor giants. The abundances of C and N in globular cluster giants (e.g., Carbon et al. 1982; Suntzeff 1981) indicates far more C $\rightarrow$ N processing in metal-poor giants than in solar metallicity giants. Furthermore, nearly all luminous metal-poor giants exhibit carbon isotope ratios less than 10 (e.g., Sneden et al. 1986 for field giants, Suntzeff & Smith 1991 for globular cluster giants). The interpretation of all these abundances is far from complete, but evidence seems to be accumulating for mixing episodes "beyond the first dredge-up" on the metal-poor giant branch before the onset of helium burning.

7. CONCLUSIONS

Observations of the lithium abundance in Population II subgiants offer strong, quantitative support to detailed theoretical models of stars evolving from the main sequence to the giant branch. For the bulk of the subgiants we observed, the amount of convective dilution observed agrees well with model predictions. Our observations provide modest support for the action of diffusion affecting the surface abundance of lithium in subdwarfs similar in mass to the Population II main-sequence turnoff. The large spread in the lithium abundance in the post-dilution subgiants suggests that the processes which affect the abundance of lithium in the interior of the star on the main sequence vary from star to star. The very low lithium abundances in the cool giants suggest that additional lithium depletion must occur following the dilution phase.

We gratefully acknowledge the assistance of the KPNO mountain staff, and we thank Charles Proffitt for communicating his predictions in advance of publication. We are also grateful to Chris Biemesderfer for his assistance in preparing the manuscript and especially the plano tables. This research was supported in part by NSF grant AST89-14917 to Sneden.

REFERENCES

Andersen, J., Gustafsson, B., & Lambert, D. L. 1984, A&A, 136, 65
Barbuy, B., Spite, F., & Spite, M. 1982, A&A, 144, 343
Bond, H. E. 1970, ApJS, 22, 117
———. 1980, ApJS, 44, 519
Briley, M. M., Hesser, J. E., & Bell, R. A. 1991, ApJ, 373, 482
Burstein, D., & Heiles, C. 1982, AJ, 87, 1165
Carbon, D. F., Barbuy, B., Kraft, R. P., Friel, E. D., & Suntzeff, N. B. 1987, PASP, 99, 335
Carbon, D. F., Langer, G. E., Butler, D., Kraft, R. P., Suntzeff, N. B., Kemper, E., Trefzger, C. F., & Romanishin, W. 1982, ApJS, 49, 207
Cayrel de Strobel, G., Hauck, B., François, P., Thevenin, F., Friel, E., Mermilliod, M., & Borde, S. 1992, A&AS, in press
Crawford, D. L. 1975, AJ, 80, 955
Dahn, C. 1992, private communication
Dearborn, D. S. P., Schramm, D. N., & Hobbs, L. M. 1992, ApJ, 394, L61
Delbouille, L., Neven, L., & Roland, G. 1973, Photometric Atlas of the Solar Spectrum from λ3000 to λ10000 Å (Liège: Institut d'Astrophysique)
Deliyannis, C. P., & Demarque, P. 1991, ApJ, 379, 216
Deliyannis, C. P., Demarque, P., & Kawaler, S. D. 1990, ApJS, 73, 21
Fitzpatrick, M. J., & Sneden, C. 1987, BAAS, 19, 1129
François, P. 1986, A&A, 160, 264
———. 1987, A&A, 176, 294
———. 1988, A&A, 195, 226
Fuhr, J. R., Martin, G. A., & Wiese, W. L. 1988, J. Phys. Chem. Ref. Data, 17, Suppl. 4., 1
Gilroy, K. K., Sneden, C., Pilachowski, C. A., & Cowan, J. J. 1988, ApJ, 327, 298
Gratton, R. G., & Ortolani, S. 1986, A&A, 169, 201
Gratton, R. G., & Sneden, C. 1987, A&A, 178, 179
———. 1988, A&A, 204, 193
———. 1991, A&A, 241, 501
Gustaffsson, B., Bell, R. A., Eriksson, K., & Nordlund, A. 1975, A&A, 42, 407
Hobbs, L. M., & Duncan, D. K. 1987, ApJ, 317, 796
Hobbs, L. M., & Thorburn, J. A. 1991, ApJ, 375, 116
Hobbs, L. M., Welty, D. E., & Thorburn, J. A. 1991, ApJ, 373, L47
Holweger, H., & Müller, E. A. 1974, Sol. Phys., 39, 19
Iben, I. 1965, ApJ, 142, 1447
Kraft, R. P., Suntzeff, N. B., Langer, G. E., Carbon, D. F., Trefzger, C. F., Friel, E., & Stone, R. P. 1982, PASP, 94, 55
Laird, J. B. 1990, private communication
Laird, J. B., Carney, B. W., & Latham, D. W. 1988, AJ, 95, 1843 (LCL)
Leep, E. M., & Wallerstein, G. 1981, MNRAS, 196, 543
Luck, R. E., & Bond, H. E. 1981, ApJ, 244, 919
———. 1985, ApJ, 292, 559
Magain, P. 1985, A&A, 146, 95
———. 1987, A&A, 179, 176
———. 1989, A&A, 209, 211
Olsen, E. H. 1983, A&AS, 54, 55
———. 1984, A&AS, 57, 443
Peterson, R. C. 1981, ApJ, 244, 989
Peterson, R. C., Kurucz, R. L., & Carney, B. W. 1990, ApJ, 350, 173
Pinnsoneault, M. A., Deliyannis, C. P., & Demarque, P. 1991, ApJ, 367, 239
Proffitt, C. P., & Michaud, G. 1991, ApJ, 371, 584
Rebolo, R., Molaro, P., & Beckman, J. E. 1988, A&A, 192, 192 (RMB)
Saxner, M., & Hammarbäck, 1985, A&A, 151, 372
Schuster, W. J., & Nissen, P. E. 1988, A&AS, 73, 225
———. 1989a, A&A, 221, 65
———. 1989b, A&A, 222, 69
Smith, G. 1981, A&A, 103, 351
Smith, G., & Raggett, D. St. J. 1981, J. Phys. B, 14, 4015
Sneden, C., Pilachowski, C. A., & VandenBerg, D. A. 1986, ApJ, 311, 826
Spite, M., Maillard, J. P., & Spite, F. 1984, A&A, 141, 56
Spite, F., & Spite, M. 1982, A&A, 115, 357
———. 1986, A&A, 163, 140
Spite, F., Spite, M., Cayrel, R., & Huille, S. 1991, in IAU Symp. 149, The Stellar Population of Galaxies, ed. B. Barbury & A. Renzini (Dordrecht: Kluwer), in press
Suntzeff, N. B. 1981, ApJS, 47, 1
Suntzeff, N. B., & Smith, V. V. 1991, ApJ, 381, 160
van Altena, W. F., Lee, J. T., & Hoffleit, E. D. 1991, The General Catalog of Trigonometric Stellar Parallaxes (1991): A Preliminary Version (New Haven: Yale Univ. Obs.)
VandenBerg, D. A. 1992, ApJ, 391, 685
Wheeler, J. C., Sneden, C., & Truran, J. W. 1989, ARA&A, 27, 279